British Journal of Pharmacology

British Journal of Pharmacology (2018) **175** 4496–4506 4496

RESEARCH PAPER

Nociceptin/Orphanin FQ (N/OFQ) conjugated to ATTO594: a novel fluorescent probe for the N/OFQ (NOP) receptor

Correspondence Professor David G. Lambert, Department of Cardiovascular Sciences, Anaesthesia, Critical Care and Pain Management, Leicester Royal Infirmary, University of Leicester, Leicester, UK. E-mail: dgl3@le.ac.uk

Received 24 April 2018; **Revised** 31 August 2018; **Accepted** 4 September 2018

M F Bird[1], R Guerrini[2], J M Willets[3], J P Thompson[1], G Caló[4] and D G Lambert[1]

[1]Department of Cardiovascular Sciences, Anaesthesia, Critical Care and Pain Management, Leicester Royal Infirmary, University of Leicester, Leicester, UK, [2]Department of Chemical and Pharmaceutical Sciences and LTTA, University of Ferrara, Ferrara, Italy, [3]Department of Molecular and Cell Biology, University of Leicester, Leicester, UK, and [4]Department of Medical Sciences, Section of Pharmacology and National Institute of Neuroscience, University of Ferrara, Ferrara, Italy

BACKGROUND AND PURPOSE

The nociceptin/orphanin FQ (N/OFQ) receptor (NOP) is a member of the opioid receptor family and is involved in a number of physiological responses, pain and immune regulation as examples. In this study, we conjugated a red fluorophore-ATTO594 to the peptide ligand N/OFQ (N/OFQ$_{ATTO594}$) for the NOP receptor and explored NOP receptor function at high (in recombinant systems) and low (on immune cells) expression.

EXPERIMENTAL APPROACH

We assessed N/OFQ$_{ATTO594}$ receptor binding, selectivity and functional activity in recombinant (CHO) cell lines. Live cell N/OFQ$_{ATTO594}$ binding was measured in (i) HEK cells expressing NOP and NOP$_{GFP}$ receptors, (ii) CHO cells expressing the hNOPGαqi5 chimera (to force coupling to measurable Ca^{2+} responses) and (iii) freshly isolated human polymorphonuclear cells (PMN).

KEY RESULTS

N/OFQ$_{ATTO594}$ bound to NOP receptor with nM affinity and high selectivity. N/OFQ$_{ATTO594}$ activated NOP receptor by reducing cAMP formation and increasing Ca^{2+} levels in CHO$_{hNOPGαqi5}$ cells. N/OFQ$_{ATTO594}$ was also able to visualize NOP receptors at low expression levels on PMN cells. In NOP-GFP-tagged receptors, N/OFQ$_{ATTO594}$ was used in a FRET protocol where GFP emission activated ATTO, visualizing ligand–receptor interaction. When the NOP$_{GFP}$ receptor is activated by N/OFQ$_{ATTO594}$, movement of ligand and receptor from the cell surface to the cytosol can be measured.

CONCLUSIONS AND IMPLICATIONS

In the absence of validated NOP receptor antibodies and issues surrounding the use of radiolabels (especially in low expression systems), these data indicate the utility of N/OFQ$_{ATTO594}$ to study a wide range of N/OFQ-driven cellular responses.

Abbreviations

DPN, diprenorphine; N/OFQ, nociceptin/orphanin FQ; NOP receptor, N/OFQ peptide receptor; PMN, polymorphonuclear cells; SB-612111, 7-[[4-(2,6-dichlorophenyl)-1-piperidinyl]methyl]-6,7,8,9-tetrahydro-1-methyl-5*H*-benzocyclohepten-5-ol hydrochloride

DOI:10.1111/bph.14504

Introduction

The nociceptin/orphanin FQ (N/OFQ) receptor (**NOP receptor**) is the newest member of the opioid receptor family (Lambert, 2008). It exhibits similar signalling mechanisms to the classical opioid receptors (**μ**, **δ** and **κ**), through activation of a $G\alpha_i$-mediated G-protein pathway (Meunier *et al.*, 1995; Reinscheid *et al.*, 1995). The NOP receptor, however, differs from the classical opioid receptors in a number of key areas. It has little to no affinity for the endogenous ligands of classical opioid receptors, nor does it have affinity for the opioid antagonist **naloxone**. Furthermore, its own endogenous ligand, **N/OFQ**, is highly selective for the NOP receptor, displaying little or no affinity for the classical opioid receptors.

Like the classical opioid receptors, NOP receptor expression has been demonstrated throughout the pain pathway, with antinociceptive actions ascribed to activation (Mollereau and Mouledous, 2000; Schroder *et al.*, 2014; Ding *et al.*, 2015). At initial identification, in mice and rat studies, it was believed that the NOP receptor had pronociceptive activity supraspinally; however, work by Ding and colleagues in non-human primates demonstrated antinociceptive activity throughout the pain pathway underscoring important interspecies differences (Ding *et al.*, 2015). The NOP receptor is expressed in a range of other non-neuronal tissues and presumed levels vary widely (Lambert, 2008). NOP-eGFP knock-in mice have been used to examine expression-function but with a neuronal focus (Ozawa *et al.*, 2015). Outside the nervous system, we and others have shown the presence of the NOP receptor in immune tissues, but due to presumed ultra-low expression, this has been suggested through PCR and modulation of immune function (Kruger *et al.*, 2006; Zhang *et al.*, 2013). While it is possible to obtain acceptable amounts of cerebral tissue to measure opioid expression through radioligand binding, the quantities of peripheral tissue available are most often inadequate for such studies.

Assessment of NOP receptor expression outside the brain is hindered by several key issues. The quantity of sample collected (e.g. immune cells) is often insufficient to perform radioligand assays, the current gold standard. Therefore, as noted above, receptor identity is often confirmed by either PCR or antibody methods. PCR detects mRNA, and these levels do not necessarily translate to functional protein (Guo *et al.*, 2008). Antibodies for GPCRs have been shown to lack the high levels of specificity required to provide evidence of expressed protein (Michel *et al.*, 2009). Previous work in our laboratory and others has demonstrated high levels of non-selectivity using commercially available antibodies (Scherrer *et al.*, 2009; Niwa *et al.*, 2012). In standard Western blotting, we demonstrated the presence of bands at the expected weight in CHO cells expressing opioid receptors as well as those that had not been transfected with the opioid receptor of interest (Niwa *et al.*, 2012). The importance of selectivity is highlighted in a study of δ (DOP) receptors (Scherrer *et al.*, 2009). In their study identifying regions of expression of δ receptors, Scherrer and colleagues demonstrated large differences between areas of expression determined by antibody when compared to δ-eGFP expressing mice (Scherrer *et al.*, 2009).

Because the NOP receptor has no affinity for classical opioid ligands and N/OFQ is highly selective for NOP receptors, labelling of N/OFQ is an exciting possibility as a replacement for radioprobes and antibodies. Here, we describe for the first time a method using N/OFQ conjugated to the highly fluorescent ATTO dye (594 nm) and show this probe has a remarkable similarity to the unlabelled peptide.

Methods

Cell culture and immune cell preparation

Hams F12 was used to culture CHO cells expressing recombinant human opioid receptors (μ, δ and κ), DMEM/F12 1:1 media were used for both CHO_{hNOP} and $CHO_{hNOPG\alpha qi5}$ (from T Costa, Istituto Superiore di Sanità, Rome, Italy) and MEM was used for HEK cells expressing the recombinant NOP (HEK_{hNOP}) receptor and $HEK_{hNOP\text{-}GFP}$. All media were supplemented with 10% FBS, 100 IU·mL^{-1} penicillin, 100-μg·mL^{-1} streptomycin and 2.5 μg·mL^{-1} fungizone. Cultures were maintained in selection media; for CHO cells containing the classical opioid receptors, 200 μg·mL^{-1} G418 was used. For HEK_{hNOP} cells, 200 μg·mL^{-1} hygromycin B was used. For both CHO_{hNOP} and $CHO_{hNOPG\alpha qi5}$ cells, 200 μg·mL^{-1} G418 and 200 μg·mL^{-1} hygromycin B were used. Recombinant cell lines were grown to confluency in T75 cm^3 flasks in supplemented media at 37°C in 5%-CO_2/humidified air. Polymorphonuclear cells (PMN) were extracted from healthy volunteers as previously described (Thompson *et al.*, 2013) and with University of Leicester volunteer research ethics committee approval. Up to 30 mL of blood was collected from each volunteer (mean age of 38; range 25–55, 4 male : 1 female) into Monovette blood collection tubes (Sardstedt, Germany) containing K-EDTA (7.5 mL blood per tube, final EDTA concentration 1.6 mg·mL^{-1}) and used within 1 h of venepuncture. PMN were extracted by centrifugation over an equal volume of Polymorphprep (Axis-Shield, Dundee). Following extraction, PMN were cleared of any potential erythrocyte contamination by using a 1:1 dilution with BD PharmaLyse (Becton, Dickinson and Company, Oxford), resuspended in Krebs buffer (0.126 M NaCl, 2.5 mM KCl, 25 mM $NaHCO_3$, 1.2 mM NaH_2PO_4, 1.2 mM $MgCl_2$, 2.5 mM $CaCl_2$) for counting and imaging. Extractions were carried out at room temperature, and the resulting cell suspension kept on ice until use (maximum 4 h). Viability and yields were quantified by Trypan Blue exclusion and counting using a haemocytometer (Strober, 2001).

Radioligand binding

Radioligand binding was quantified in CHO cells stably transfected with μ, δ, κ and NOP receptors. Twenty to forty micrograms of membrane protein were incubated in 0.5 mL wash buffer (50 mM Tris–HCL, pH 7.4 KOH with the addition of 0.5% BSA), ~0.8 nM **[^{3}H]-diprenorphine** (DPN; for classical opioid membranes) or ~0.8 nM [^{3}H]-N/OFQ (for CHO_{hNOP} membranes), varying concentrations (1 pM–10 μM) of the control ligand or $N/OFQ_{ATTO594}$. Non-specific binding was measured in the presence of 10 μM

naloxone (μ, δ, κ receptors) or 1 μM of N/OFQ (NOP receptor). Samples were incubated at room temperature for 1 h. Reactions were terminated by vacuum filtration onto polyethylenimine-soaked Whatman GF/B filters, using a Brandel harvester (Bird *et al.*, 2015).

cAMP inhibition assay

$HEK_{hNOP\text{-}GFP}$ cells were suspended in Krebs/HEPES buffer, pH 7.4 NaOH containing **forskolin** (1 μM) and **IBMX** (1 mM). Both the control ligand (unlabelled N/OFQ) and the $N/OFQ_{ATTO594}$ were included in a range of concentrations (0.1 pM–1 μM) and incubated at 37°C for 15 min. Reactions were terminated through the initial addition of 20 μL 10 M HCl, followed by 20 μL 10 M NaOH and 200 μL 1 M Tris–HCl (pH 7.4) to equilibrate the pH. Reactions were centrifuged at 16 000× *g* and supernatant collected. The supernatant was incubated with **[^{3}H]-cAMP** and an in-house prepared binding protein overnight at 4°C. Charcoal/BSA suspension was added and the reaction centrifuged at 16 000× *g*, following which, samples of the supernatant were counted as previously described (Kitayama *et al.*, 2007).

Confocal microscopy

At confluence, NOP expressing cells were passaged onto ethanol-sterilized 28 mm Menzel glaser #1-coverslips (Thermo Scientific, Loughborough, UK) and incubated for 24 h before use. Cells were perfused with Krebs buffer, pH 7.4 at 4°C using a temperature controller and microincubator (PDMI-2 and TC202A; Burleigh, Digitimer, Cambridge, UK) when studying ligand–receptor binding, while in functional studies (internalization of the ligand–receptor complex), cells were incubated at 37°C. Where used, immune cells were plated onto coverslips pretreated with Celltak™ (1 $\mu g \cdot mL^{-1}$) (Sigma, UK) and incubated at 37°C for 1 h, before being washed in ice-cold Krebs buffer.

$N/OFQ_{ATTO594}$ was injected onto coverslips, allowing for a range of concentrations to be measured (1 pM−100 nM, cumulatively), following which, images were captured using a Nikon Eclipse C1Si microscope (Surrey, UK), using an oil immersion 60× objective. $N/OFQ_{ATTO594}$ was allowed to incubate for 5 min at 4°C before the coverslip was washed with ice-cold Krebs buffer. Following this incubation period, HEK_{hNOP} cells were imaged using the 594 nm wavelength laser, with images collected by the Nikon C1Si software. $HEK_{hNOP\text{-}GFP}$ and $CHO_{hNOPg\alpha q/i5}$ cells were imaged sequentially using the 594 nm wavelength followed by 488 nm to assess $N/OFQ_{ATTO594}$ and GFP/Fluo4-AM respectively, 10 s per frame. In order to determine specificity of binding, the NOP antagonist **SB-612111** (1 μM) was pre-incubated in desired cells for 15 min before addition of $N/OFQ_{ATTO594}$. PMN were incubated with 100 nM $N/OFQ_{ATTO594}$ and, following washing with ice-cold Krebs, were imaged using the 594 nm wavelength laser. In all experiments, the laser and gain settings were maintained constant. For experiments with $N/OFQ_{ATTO594}$ alone, settings were 37% 594 nm laser power, 7.10 gain-red channel. In experiments including Fluo4-AM stained cells (see below), 488 nm laser, an 18% power setting with 7.15 gain setting was used. Internalization studies were performed using 100 nM $N/OFQ_{ATTO594}$ at 1 and 15 min time points (488 nm/594 nm wavelengths) in $HEK_{hNOP\text{-}GFP}$ cells. FRET studies were undertaken by measuring the binding of $N/OFQ_{ATTO594}$ to $HEK_{hNOP\text{-}GFP}$. NOP-GFP receptors were stimulated using a 488 nm laser, and measurements were made using the RED (594 nm) filter channel (Wallrabe *et al.*, 2003). In order to confirm FRET-pairing, several additional controls were performed (Snapp and Hegde, 2006). $N/OFQ_{ATTO594}$ (100 nM) was incubated on HEK_{hNOP} cells (not expressing the GFP fluorophore) and measured using 488 nm laser. Furthermore, photobleaching of the ligand was performed, after binding to $HEK_{hNOP\text{-}GFP}$, by exposing it to 594 nm laser until fluorescence was undetectable, following which levels of GFP fluorescence intensity were measured. While GFP and ATTO594 may not be specifically designed as an optimum FRET pair, there is still significant crossover as demonstrated by spectra analyser data.

$CHO_{hNOPG\alpha qi5}$ functional assays

In experiments using $CHO_{hNOPG\alpha qi5}$ cells (Camarda and Calo, 2013), the cells were incubated with 1 μM Fluo4-AM for 45 min in Krebs buffer, following which they were washed for 3 min in 4°C Krebs *via* the perfusion system. A series of experiments were also performed at the physiological temperature of 37°C. $N/OFQ_{ATTO594}$ (100 nM) was perfused while the cells were monitored under the confocal microscope [imaging using both 488 nm laser (Fluo4-AM) and 594 nm laser ($N/OFQ_{ATTO594}$)].

Data analysis

All data are the mean of five experiments ± SEM as appropriate. Specimen confocal data sets are presented. All confocal images were analysed using ImageJ with resulting data analysed using GraphPad Prism-v7. To measure corrected cell fluorescence, the formula, Corrected total cell fluorescence = Integrated density − (Area of selected cell × Mean fluorescence of background readings), was used to determine levels of $N/OFQ_{ATTO594}$ as previously described (Burgess *et al.*, 2010). In internalization studies, ImageJ tool plot profile was used to determine the position of $N/OFQ_{ATTO594}$ and/or NOP_{GFP} relative to the cell membrane (Wallrabe *et al.*, 2003). All experiments were performed unblinded.

Materials

$N/OFQ_{ATTO594}$, N/OFQ, dermorphin, Leu-enkephalin and **dynorphin-A** were synthesized in-house at the University of Ferrara. Tritiated diprenorphine ([^{3}H]-DPN) and tritiated N/OFQ ([^{3}H]-N/OFQ) were purchased from Perkin Elmer (UK). Details of the synthesis of $N/OFQ_{ATTO594}$ can be found in the Supporting Information Data S1 and Figures S1–S3.

Nomenclature of targets and ligands

Key protein targets and ligands in this article are hyperlinked to corresponding entries in http://www.guidetopharmacology.org, the common portal for data from the IUPHAR/BPS Guide to PHARMACOLOGY (Harding *et al.*, 2018), and are permanently archived in the Concise Guide to PHARMACOLOGY 2017/18 (Alexander *et al.*, 2017).

Results

Binding selectivity and affinity

Selectivity for N/OFQ$_{ATTO594}$ was measured in CHO cells expressing human μ, δ, κ and NOP receptors. In CHO$_{hNOP}$ cells, N/OFQ$_{ATTO594}$ displaced [^{3}H]-N/OFQ in a concentration dependent and saturable manner (pK$_i$: 9.21), which was not significantly (Student's *t*-test) different from unlabelled N/OFQ (9.37) (Figure 1). N/OFQ$_{ATTO594}$ failed to displace [^{3}H]-DPN in cells expressing μ, δ or κ receptors (Figure 1). In HEK$_{hNOP}$ cells, N/OFQ$_{ATTO594}$ also displaced [^{3}H]-N/OFQ in a concentration dependent and saturable manner (pK$_i$ 9.14 ± 0.13; n = 5), which was not significantly (Student's *t*-test) different from unlabelled N/OFQ (pK$_i$: 9.34 ± 0.08; n = 5). A range of concentrations of N/OFQ$_{ATTO594}$ were added to HEK cells expressing the NOP receptor and binding measured using 594 nm laser on a confocal microscope (Figure 2). N/OFQ$_{ATTO594}$ bound in a concentration-dependent and saturable manner, producing a pK$_d$ of 9.51 ± 0.18 (n = 5; Figure 2). In HEK cells expressing GFP-tagged NOP (HEK$_{hNOP-GFP}$) cells, N/OFQ$_{ATTO594}$ bound to NOP with an affinity (pK$_i$) of 8.98 ± 0.06 in displacement binding assays using [^{3}H]-N/OFQ as the radiolabel (Figure 3). When binding affinity was assessed directly using confocal microscopy, N/OFQ$_{ATTO594}$ produced a binding affinity (pK$_d$) of 8.53 ± 0.34, which was not significantly (Student's *t*-test) different from that determined by displacement (Figure 3A–I, J). In confocal experiments, pre-incubation with SB-612111 abolished N/OFQ$_{ATTO594}$ binding.

Pharmacological activity

In order to determine whether conjugation of the fluorescent tag had any effect on functional activity, cAMP inhibition assays were performed (Figure 3K). The control ligand, unlabelled N/OFQ produced a pEC$_{50}$ of 10.23 ± 0.25 and E$_{max}$ of 85.43 ± 2.70% inhibition of forskolin-stimulated cAMP formation. N/OFQ$_{ATTO594}$ produced a pEC$_{50}$ of 9.73 ± 0.29 and E$_{max}$ of 89.30 ± 2.04%. There was no significant (Student's *t*-test) difference in functional activity of N/OFQ$_{ATTO594}$ when compared to N/OFQ (Figure 3K).

In experiments performed at 4°C, 100 nM N/OFQ$_{ATTO594}$ was added to CHO$_{hNOPG\alpha qi5}$ cells loaded with the calcium indicator, Fluo4-AM (Figure 4A–D). An increase in red fluorescence can be seen around the membrane after addition of N/OFQ$_{ATTO594}$, following which an increase in green fluorescence can be seen indicating activation of the G$_{\alpha qi5}$-coupled NOP receptor and subsequent increase in cytosolic calcium (Figure 4A–D and Supporting Information Video S1). The kinetics of the rise in Ca^{2+} is slow as the experiment was performed at 4°C. Binding of N/OFQ$_{ATTO594}$ at 37°C led to a more rapid increase of Ca^{2+} (Figure 4E–G).

Low expression systems

Immune cells are known to express NOP mRNA and do not bind radiolabelled N/OFQ, but their function is modulated in response to N/OFQ. We next used N/OFQ$_{ATTO594}$ to determine whether we could detect NOP at low levels of expression. Human PMN cells separated from healthy

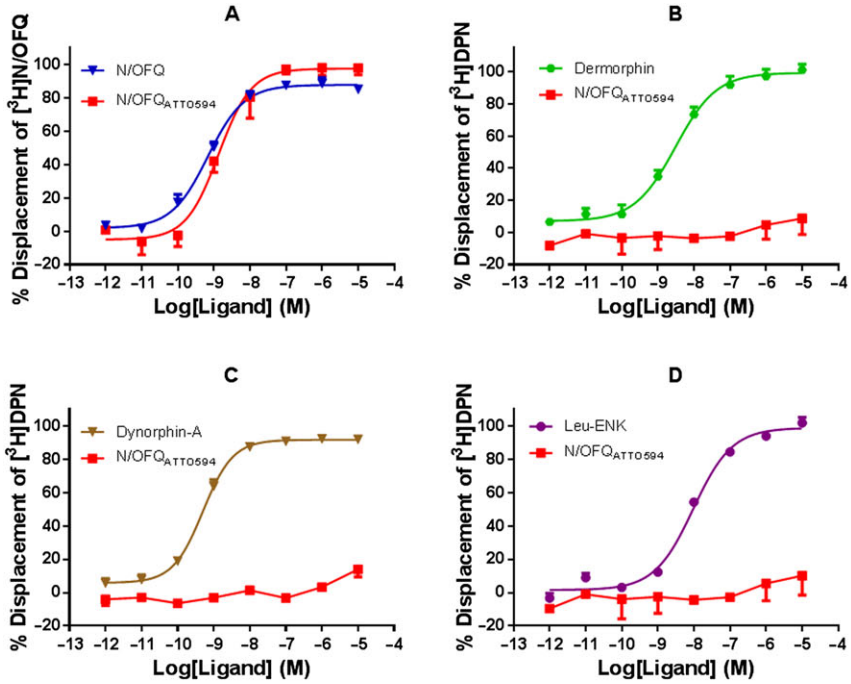

Binding Affinity (pK$_i$)	Control	N/OFQ$_{ATTO594}$
CHO$_h$NOP	9.37 (±0.09)	9.21 (±0.12)
CHO$_h$μ	8.51 (±0.11)	None
CHO$_h$δ	8.07 (±0.05)	None
CHO$_h$κ	9.30 (±0.04)	None

Figure 1

Displacement of [^{3}H]-N/OFQ in CHO$_{hNOP}$ cell membranes by a range of concentrations of N/OFQ and N/OFQ$_{ATTO594}$ (A). Displacement of [^{3}H]-DPN in CHO$_{h\mu}$ cell membranes by a range of concentrations of dermorphin and N/OFQ$_{ATTO594}$ (B). Displacement of [^{3}H]-DPN in CHO$_{h\kappa}$ cell membranes by a range of concentrations of dynorphin-A and N/OFQ$_{ATTO594}$ (C). Displacement of [^{3}H]-DPN in CHO$_{h\delta}$ cell membranes by a range of concentrations of Leu-enkephalin and N/OFQ$_{ATTO594}$ (D). Displacement binding affinities for N/OFQ$_{ATTO594}$ and control ligands are summarised in the table (NOP: N/OFQ; μ: dermorphin; δ: Leu-enkephalin; κ: dynorphin-A). Data are the mean ± SEM of five experiments.

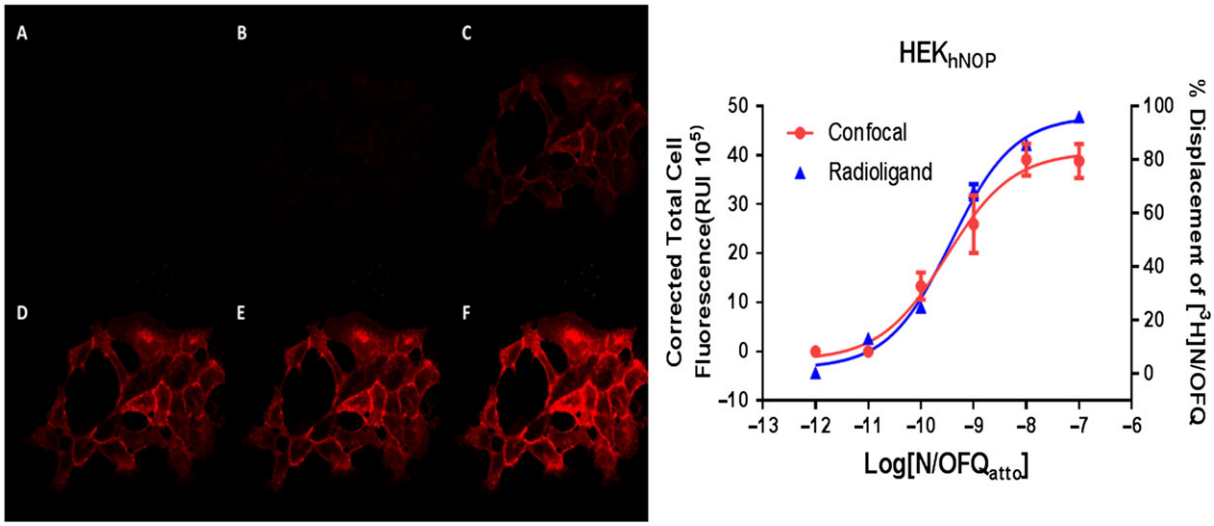

Figure 2

Concentration-dependent binding of N/OFQ$_{ATTO594}$ to HEK$_{hNOP}$ cells using confocal microscopy and stimulation with 594 nm laser and [^{3}H]-N/OFQ. On the left representative images of the binding of various concentrations (A: 1 pM; B: 10 pM; C: 100 pM; D: 1 nM; E: 10 nM; F: 100 nM) of N/OFQ$_{ATTO594}$ using confocal microscopy. On the right are the binding curves analysed as in methods overlayed with data from a [^{3}H]-N/OFQ displacement analysis; data are mean ± SEM for five experiments. Confocal experiments were performed at 4°C while radioligand binding assays were performed at room temperature.

volunteers were seeded onto cover slips. At a temperature of 4°C, N/OFQ$_{ATTO594}$ (100 nM) binding was observed (Figure 3L), indicating the presence of NOP receptors. Furthermore, pre-incubation with unlabelled N/OFQ (1 μM; Figure 3M) or the selective NOP antagonist SB-612111 (1 μM; Figure 3O) blocked the binding of N/OFQ$_{ATTO594}$. The addition of naloxone (1 μM) had no effect on N/OFQ$_{ATTO594}$ binding (Figure 3P); this is consistent with the selectivity of binding of N/OFQ$_{ATTO594}$. In a further experiment to confirm NOP expression, PMN cells were pre-incubated with N/OFQ before the addition of 100 nM N/OFQ$_{ATTO594}$ (Figure 3R), demonstrating no binding of N/OFQ$_{atto594}$. Cells were washed for several minutes in ice-cold Krebs, following which 100 nM N N/OFQ$_{ATTO594}$ was added for a second time. In this instance, binding was restored (Figure 3S). Brightfield images are shown in panels N, Q and T.

NOP receptor internalization

We then used N/OFQ$_{ATTO594}$ to track NOP receptor internalization. Binding was initially measured at 4°C using 100 nM of N/OFQ$_{ATTO594}$ in HEK$_{hNOP\text{-}GFP}$ cells (Figure 5A, C and E) clearly demonstrating a localization of N/OFQ$_{ATTO594}$ (Figure 5C) on the cellular membrane with GFP-tagged NOP (A and overlay E). Following a temperature increase to 37°C, N/OFQ$_{ATTO594}$ is seen to mobilize within the cell, away from the cell membrane (D). These pools of N/OFQ$_{ATTO594}$ are shown to co-localize with internalized NOP-GFP (B and overlay F). Using ImageJ line analysis (dotted line in A–F), it is possible to assess the change in fluorescence at different time points across the cell after binding of N/OFQ$_{ATTO594}$ (Figure 5G) and the subsequent localization of NOP-GFP (Figure 5H).

Because of the close proximity formed between ligand–receptor complexes (Figure 6M), a FRET stimulation was performed in HEK$_{hNOP\text{-}GFP}$ cells using N/OFQ$_{atto594}$. When the receptor complex was formed, the 488 nm laser was used (Figure 6A–D), while filters in the red channel were viewed. In the absence of N/OFQ$_{ATTO594}$, no image was obtained (Figure 6B). After administration of 100 nM N/OFQ$_{ATTO594}$, a clear image demonstrating areas of interaction of NOP$_{GFP}$-N/OFQ$_{ATTO594}$ was seen (Figure 6C), indicating FRET. The overlap of NOP$_{GFP}$ and N/OFQ$_{ATTO594}$ can be seen in an overlaid composite image (Figure 6D). In order to confirm FRET-pairing, 100 nM N/OFQ$_{ATTO594}$ was incubated with HEK$_{hNOP}$ cells (not expressing GFP), following which detection of binding was attempted using the 488 nm wavelength laser (Figure 6E). N/OFQ$_{ATTO594}$ was not stimulated by the laser in this environment. Binding of N/OFQ$_{ATTO594}$ to the surface was confirmed by stimulation with 594 nm laser (Figure 6F). A second control experiment was performed, whereby 100 nM N/OFQ$_{ATTO594}$ was incubated with HEK$_{hNOP\text{-}GFP}$ cells and exposed to prolonged stimulation through 594 nm laser wavelengths (Figure 6G–L). This produced photobleaching of the ligand (Figure 6J). The level of GFP fluorescence was taken before and after photobleaching and demonstrated that the corrected total cell fluorescence of GFP had a statistically significant increase from 0.78 ± 0.11 to 1.11 ± 0.17 (Student's *t*-test; $P < 0.05$) (Figure 6N).

Discussion

In this study, we report the synthesis and use of a novel fluorescent probe for the NOP receptor, N/OFQ$_{ATTO594}$. We have conjugated ATTO594 to the highly selective endogenous NOP ligand N/OFQ, and this new ligand retains high NOP selectivity (over classical opioid receptors) and full agonist activity in (i) cAMP inhibition experiments performed in cells expressing NOP receptors (Kitayama *et al.*, 2007), (ii) Ca^{2+}

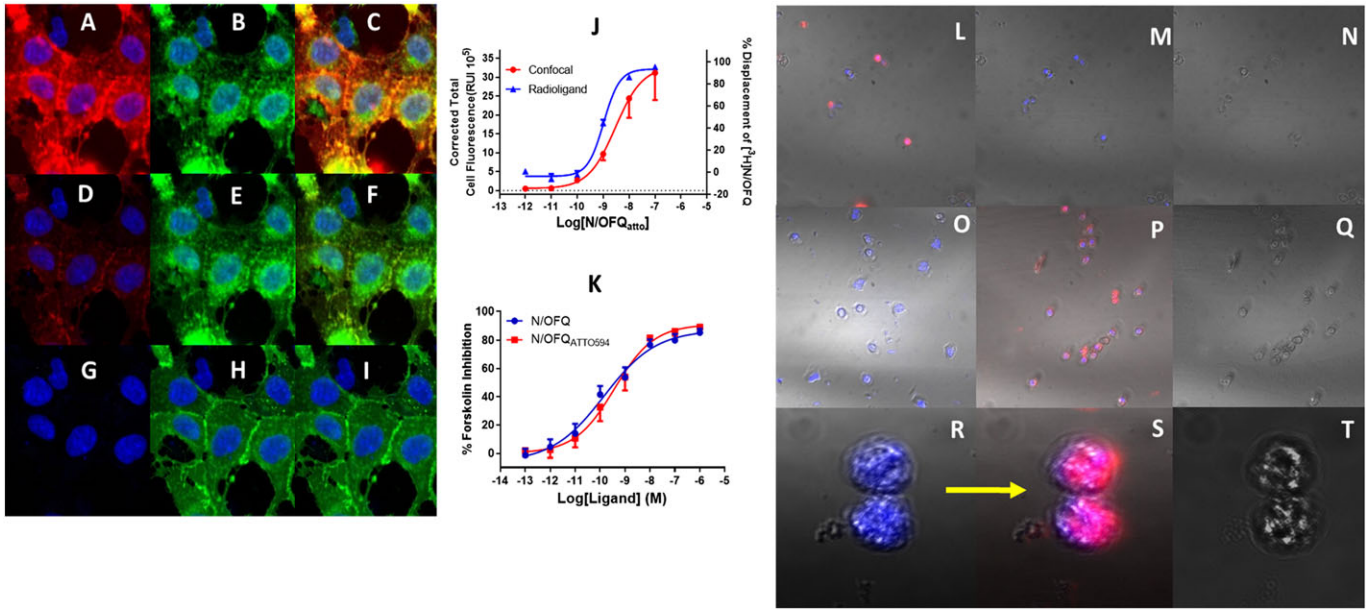

Figure 3

A–C: Binding of 100 nM N/OFQ$_{ATTO594}$ in HEK$_{hNOP\text{-}GFP}$ split into the red channel (A) with N/OFQ$_{ATTO594}$ binding, (B) the green channel to identify NOP$_{GFP}$ tagged receptors and (C) a composite image demonstrating the interaction between N/OFQ$_{ATTO594}$ and NOP$_{GFP}$. (D–F) Binding of 1 nM of N/OFQ$_{ATTO594}$ split into the red channel (D) showing N/OFQ$_{ATTO594}$ binding, (E) the green channel identify NOP$_{GFP}$ tagged receptors and (F) a composite image demonstrating overlapping binding of N/OFQ$_{ATTO594}$ with NOP$_{GFP}$. (G–I) Binding of 1 pM of N/OFQ$_{ATTO594}$ showing split into the red channel (G) showing N/OFQ$_{ATTO594}$ binding, (H) the green channel identify NOP$_{GFP}$ tagged receptors and (I) a composite image demonstrating no binding of N/OFQ$_{ATTO594}$ to NOP$_{GFP}$. Nucleus is blue with DAPI stain. (J) Comparison between a radioligand displacement binding curve (using ^{3}H-N/OFQ at room temperature) and saturation curve measurement obtained from confocal microscopy. Data are mean ± SEM for five experiments. (K) Functional analysis of N/OFQ$_{atto}$ activity (red) in a cAMP inhibition assay when compared to unlabelled N/OFQ. Data are mean ± SEM for five experiments performed at 37°C. (L) The ability of 100 nM N/OFQ$_{ATTO594}$ to bind and visualize low expression systems is demonstrated in human PMN at 4°C. This binding can be disrupted by both unlabelled N/OFQ (1 μM) (M) and SB-612111 (1 μM) (O). Furthermore, the classical opioid antagonist naloxone (1 μM) is unable to inhibit N/OFQ$_{ATTO594}$ binding (P). In the enlarged image, unlabelled N/OFQ is pre-incubated with PMN cells to occupy NOP receptors, before addition of 100 nM N/OFQ$_{ATTO594}$ (R) [and as in M]), again inhibiting binding of the fluorescent ligand. After washing in Krebs to 'clear' the receptor for 10 min, 100 nM N/OFQ$_{ATTO594}$ is able to bind to the surface of the PMN (S) [and as in L]). Bright field images for the accompanying experiments are shown in (N), (Q) and (T). All PNM data have been repeated for a total of five experiments. All confocal experiments were undertaken at 4°C.

mobilisation experiments in cells co-expressing NOP and chimeric G proteins (Camarda and Calo, 2013) and (iii) receptor internalization studies (Arttamangkul *et al.*, 2000). N/OFQ$_{ATTO594}$ was visibly detected over a range of concentrations when studied using confocal microscopy with sufficient sensitivity to determine a pK$_d$; this did not differ from values obtained using the standard [^{3}H]-N/OFQ binding protocol. The nM affinity reported here, coupled with the high intrinsic brightness of ATTO594 allows for the visualization of NOP receptors in low expression systems, PMN. Use of cells expressing NOP receptors coupled to GFP allows further use of N/OFQ$_{ATTO594}$ in a FRET-based assay to document ligand–receptor interaction. Finally, this new ligand is well suited to studies of receptor internalization, and when coupled with a GFP tagged receptor, it should be possible to track both receptor and ligand fate following binding and activation and unbinding.

Because N/OFQ is an agonist for the NOP receptor, we have measured binding in confocal experiments at 4°C. At the more conventional 37°C, there would be substantial activation and loss of cell surface receptors (see below) as we have shown previously (Hashimoto *et al.*, 2002; Barnes *et al.*, 2007). The assessment of binding affinity would not be affected by temperature (Ahmadi *et al.*, 2014) provided the ligand–receptor interaction was allowed to reach equilibrium, and we have a consistent assessment of affinity in HEK$_{NOP}$ and HEK$_{hNOP\text{-}GFP}$. These values were not different from the native peptide, but coupling of NOP to GFP has reduced binding affinity. At 4°C, there is the potential for non-equilibrium and an ideal solution would be to confirm affinity using association/dissociation time courses. In this paradigm, (i) the chamber floods with 'free' label making it impossible to determine bound ligand (i.e. separate from free) and (ii) experiments would be very long as the label is added cumulatively with the potential for internalization. We are reassured that our estimate of K_D is sensible as the values overlap with [^{3}H]-N/OFQ binding in membranes, and cognisant of the issues, we used two cell lines to confirm that all values are in good agreement. Measuring binding at the lower temperature followed by rapid warming allows the kinetics of internalization to be assessed. Despite measuring binding at 4°C, it is still possible to track receptor activation, at least at the level of Ca^{2+} in cells co-expressing NOP and $G_{\alpha qi5}$ chimeric G-protein. A similar shaped but more rapid response is also seen at 37°C. The kinetics at the lower temperature are substantially slower than we have previously reported

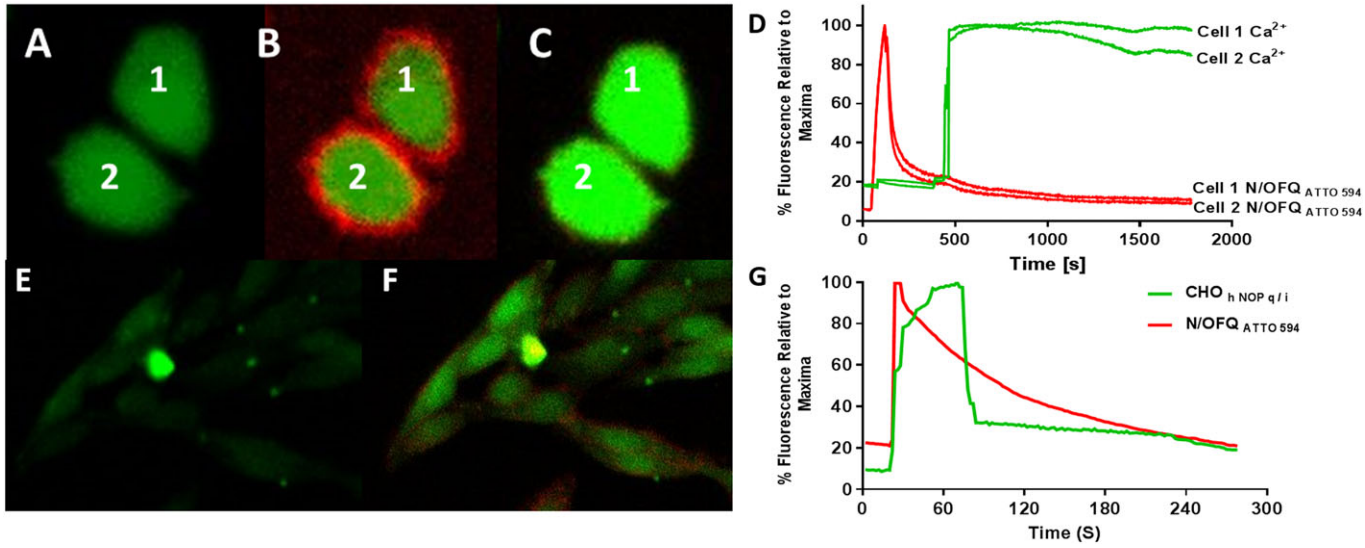

Figure 4

Live cell binding of $N/OFQ_{ATTO594}$ and subsequent stimulation in $CHO_{hNOPG\alpha qi5}$ cells. Fluo4-AM loaded $CHO_{hNOPG\alpha qi5}$ cells at 4°C (A) are incubated with 100 nM $N/OFQ_{ATTO594}$ after 30 s (B) leading to release of calcium (cells labelled 1 and 2) (B and C). The process is demonstrated in the Supporting Information Video S1. This video has been created through ImageJ (eight frames per second), with $N/OFQ_{ATTO594}$ added after 15 s, with the entirety of the video covering approximately 4.5 min. (D) A representative figure demonstrating $N/OFQ_{ATTO594}$ binding to $CHO_{hNOPG\alpha qi5}$ cells at 4°C and the increase in Ca^{2+}. Note: red is $N/OFQ_{ATTO594}$ binding and green is Ca^{2+}. Fluo4-AM loaded $CHO_{hNOPG\alpha qi5}$ cells at 37°C (E) are incubated with 100 nM $N/OFQ_{ATTO594}$ after 30 s, which leads to a prompt increase in binding and calcium (small field of cells; F). (G) A representative figure demonstrating binding of $N/OFQ_{ATTO594}$ at 37°C and increase in Ca^{2+}. Note: red is $N/OFQ_{ATTO594}$ binding and green is Ca^{2+}. These data are representative of $n = 5$.

for experiments performed at the higher temperature in population measurements, but the shape of the response is similar at all temperatures (Camarda and Calo, 2013).

Studies with GPCRs are, in general, hampered by lack of good antibodies for use in Western blotting (Hamdani and van der Velden, 2009; Jensen *et al.*, 2009; Pradidarcheep *et al.*, 2009; Berahovich *et al.*, 2010; Cecyre *et al.*, 2014; Talmont and Mouledous, 2014). This is likely due to the high degree of structural conservation both between families and more specifically in members of the same family, for example, the opioid family. Use of knockout tissue controls is often lacking, and as such, the validity of work using these probes could be questioned; this is not the case with our highly selective $N/OFQ_{ATTO594}$. A more conventional strategy is to use radiolabelled probes. For NOP, this includes [^{3}H]-N/OFQ (McDonald *et al.*, 2003), [^{3}H]-N/OFQ(1–13)-NH_2 (Hashiba *et al.*, 2002), [^{125}I]-N/OFQ (Singh *et al.*, 2013) and [^{3}H]-UFP-101 [(Bird *et al.*, 2016); their use is best employed where there is favourable access to tissue or where radioligand specific activity is high (e.g. with ^{125}I). There are a series of elegant studies using radioligands for NOP in autoradiographic protocols (Slowe *et al.*, 2001), but these retain the same issues regarding expression. Radioligands are in general not suited to use in tissues with presumed low expression, for example, vas deferens (Guerrini *et al.*, 1998) and on immune cells (see below).

A further approach to track receptor fate is to use fluorescently labelled receptors, as we have done here with NOP_{GFP} receptors. An elegant example of how this can be used comes from the work of Evans *et al.* (2010). In this study, the authors produced fluorescently labelled isoforms of μ, δ and κ along with NOP receptors. Using a confocal paradigm, they went on to address receptor dimerization. They measured the degree of colour overlap in a manner similar to our data set examining overlap of GFP and ATTO to visualize ligand–receptor interaction either in the 'conventional' sense or in a FRET protocol. They conclusively showed that NOP was capable of hetero-dimerization with all members of the opioid family (Evans *et al.*, 2010).

In this study, as controls for FRET, we ensured that 488 nm wavelength alone did not stimulate ATTO (HEK_{NOP} cells without GFP tag) and in the presence of the GFP tag SB-612111 (NOP antagonist) inhibits any FRET response. This indicates (i) ATTO is being stimulated by the emission spectra of GFP not through the laser, and (ii) it must be bound to the receptor to see the response, that is, locality which is the basis of FRET. Furthermore, photobleaching of the acceptor ($N/OFQ_{ATTO594}$) leads to increased fluorescence measurements of GFP, a positive indicator of FRET pairing (Snapp and Hegde, 2006).

It has been known for many years that opioids are immune modulators (Vallejo *et al.*, 2004), recently reviewed by Plein and Ritter (2018). The site of immune modulation is contentious, and we have reviewed this topic recently (Al-Hashimi *et al.*, 2013). Opioids could interact directly with the immune cell, modulate the activity of the hypothalamic–pituitary–adrenal axis and/or exert central actions involving glia (Hutchinson *et al.*, 2011). The expression of opioid receptors on immune cells is the most contentious. There is well known modulation of immune cell activity (migration and cytokine release) (Liang *et al.*, 2016), but we have failed to detect classical opioid (μ, δ and κ) receptor mRNA in

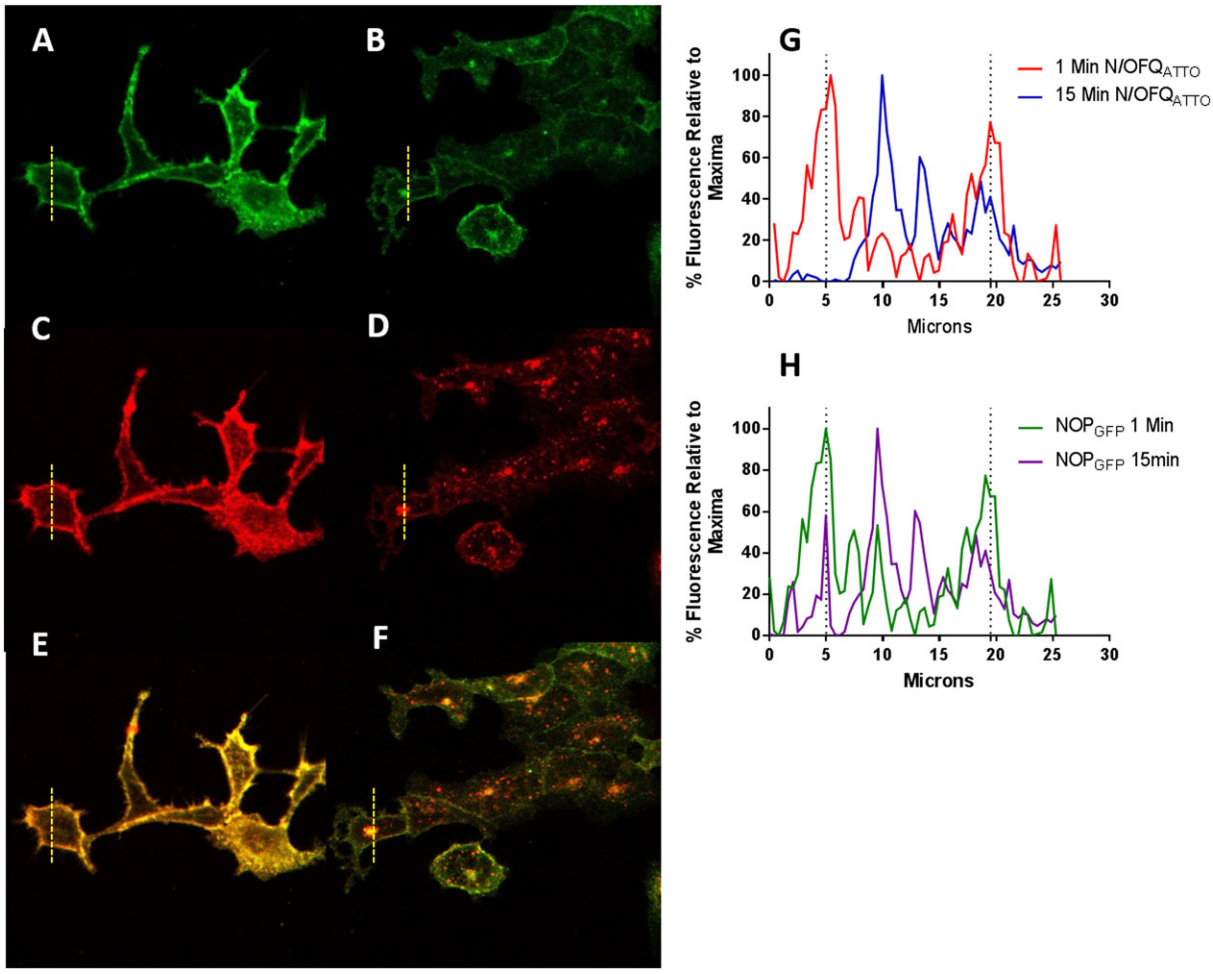

Figure 5

Use of $N/OFQ_{ATTO594}$ and NOP_{GFP} to examine cell surface receptor expression. All images depict $HEK_{hNOP\text{-}GFP}$ cells. Panels A, C and E are at 4°C and measured 1 min after ligand addition while panels B, D and F are at 37°C, 15 min after ligand addition. Green channel for NOP_{GFP} is in A and B; red channel for $N/OFQ_{ATTO594}$ is in C and D, and the overlap is in E and F. Panel G shows a representative graph of the initial binding of $N/OFQ_{ATTO594}$ (red; 1 min after adding $N/OFQ_{ATTO594}$) and subsequent change in localization (blue; 15 min after adding $N/OFQ_{ATTO594}$). Panel H shows a representative graph of initial location of NOP_{GFP} (green; 1 min after adding $N/OFQ_{ATTO594}$) and subsequent change in localization (purple; 15 min after adding $N/OFQ_{ATTO594}$) In (G and H), the dotted lines are used to indicate the position of the membrane with the cell interior between the two.

any peripheral circulating immune cells (Al-Hashimi *et al.*, 2016). This is not consistent with the modulation of function, and in this area particularly, the lack of reliable antibodies for Western blot is a major disadvantage. It is possible that opioids could be working *via* a non-opioid mechanism such as TLR4 receptors (Franchi *et al.*, 2012), or there could be differences in circulating and resident immune cells. There is no evidence for the latter in the area of opioid pharmacology. What is clear is that all circulating immune cells that we have examined to date expressed mRNA for NOP receptors, and we and others have been able to report modulation of immune function (Singh *et al.*, 2016). We have attempted to measure [^{125}I]-N/OFQ and [^{3}H]-N/OFQ binding to membranes from circulating mixed human immune cells (predominantly polymorphs). These experiments failed despite the use of relatively large amounts of membrane tissue, and we infer this is due to ultra-low expression. After careful characterization in high expressing recombinant systems, in the present study, we went on to use $N/OFQ_{ATTO594}$ in polymorphs from human volunteers and were able to detect binding. The small size of these immune cells (relative to the recombinants) and resolution of the microscope are limiting factors in pictorially demonstrating membrane location (see Supporting Information Figure S4). However, we were able to detect binding that could be blocked by pre-occupying NOP with N/OFQ or the selective NOP antagonist SB-612111 indicating both selectivity of binding to NOP and membrane location. Moreover, unlabelled N/OFQ could be effectively washed and replaced with $N/OFQ_{ATTO594}$. These results demonstrate that NOP receptor mRNA measured in PCR experiments is effectively translated into protein capable of binding N/OFQ and, unlike classical opioid receptors, provides a target to explain the observed immune modulation.

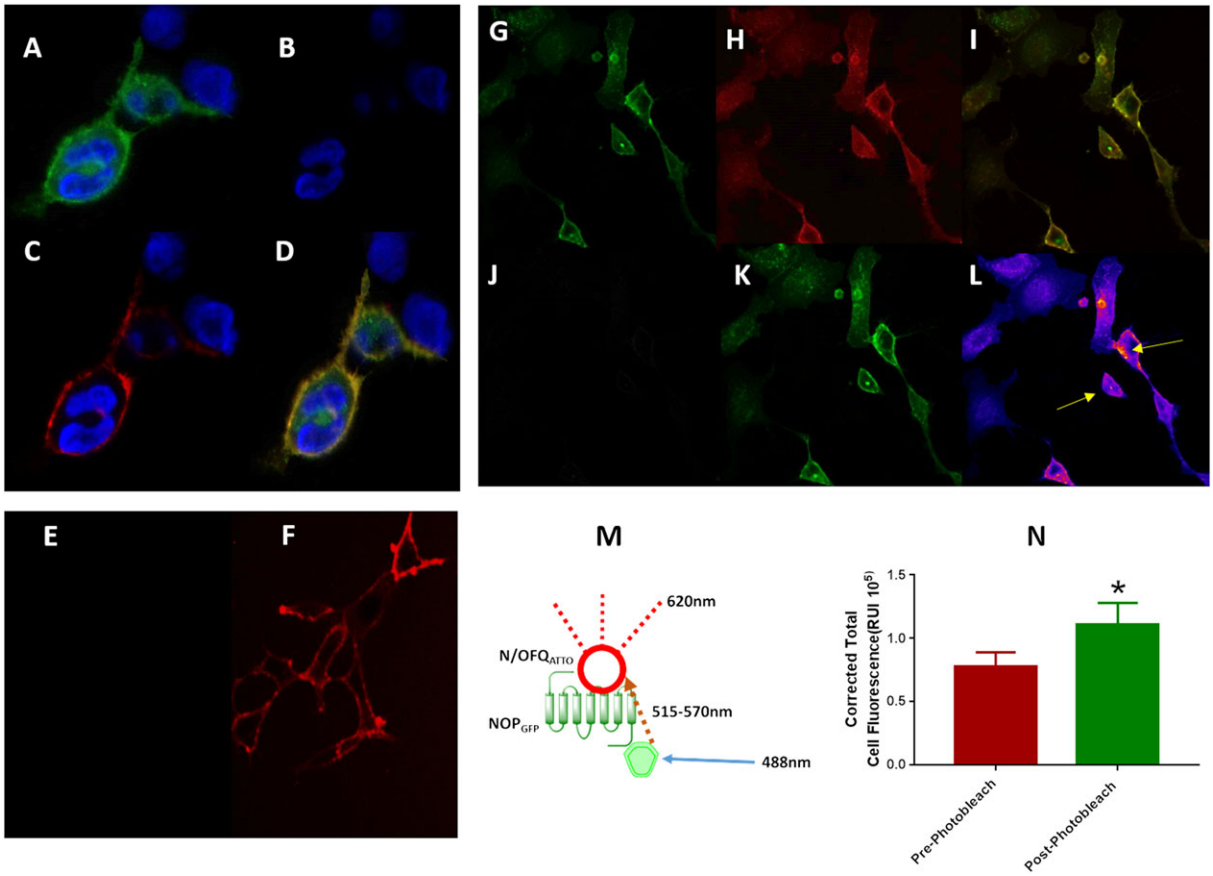

Figure 6

$N/OFQ_{ATTO594}$ can be activated when in close proximity to GFP attached to the NOP receptor (FRET), as described in the cartoon in the middle of the figure (M). (A) Visualizes the NOP_{-GFP} receptors stimulated by the 488 nm laser in the green filter window. (B) Demonstrates no 'leak' of fluorescence into the red window when using the green laser in the absence of $N/OFQ_{ATTO594}$. Upon addition of 100 nM $N/OFQ_{ATTO594}$, the ligand is stimulated through FRET pairing (C) to fluoresce when in close proximity to the NOP_{GFP} receptors. Signals are overlapped in (D). (E) In order to confirm FRET pairing, the 488 nm laser was used in conjunction with HEK_{hNOP} cells (no fluorescent linker present) to again demonstrate lack of activation of $N/OFQ_{ATTO594}$. (F) Binding of $N/OFQ_{ATTO594}$ was confirmed using 594 nm laser. Photobleaching of the acceptor molecule is a further method to confirm FRET pairing. $HEK_{hNOPGFP}$ cells (G) were labelled with 100 nM $N/OFQ_{ATTO594}$ (H) with binding of the receptor-ligand complex shown as a composite image (I). N/OFQ_{ATTO} was exposed to 594 nm light until photobleaching was achieved (J) at which point changes in NOP_{GFP} fluorescence were measured (K) with the heatmap indicating increases of fluorescence shown and highlighted by arrows (blue: low and red: high) (L). (N) Average increase in NOP_{GFP} fluorescence after photobleaching of $N/OFQ_{ATTO594}$; $P < 0.05$ Students t-test. Data are the mean of eight experiments.

Upon activation opioid receptors are internalized in an arrestin-driven fashion (Williams *et al.*, 2013). This is a fairly standard mechanism utilized by a number of GPCRs (Peterson and Luttrell, 2017) and leads to reduced cellular responsiveness or desensitization. For the NOP receptor, we have used a BRET protocol (using Renilla luciferase-NOP and Renilla GFP on arrestin) to show efficient arrestin coupling (Malfacini *et al.*, 2015). We have used radioligand binding to measure loss of cell surface NOP receptors following a desensitizing challenge. These latter studies were in high expressing (Hashimoto *et al.*, 2002) or inducible expressing (Barnes *et al.*, 2007) systems. The issues with these types of experiments is complete removal of the desensitizing challenge as any residual receptor occupancy would effectively reduce apparent density leading to an erroneous conclusion as to loss of receptors. The fluorescent probe we have designed, as an agonist itself, overcomes these problems. In this study, we show that receptors on the cell surface (GFP tagged) with N/OFQ (ATTO) bound leave the cell surface together (line analysis); ligand and receptor appear to co-localize inside the cell. Use of $N/OFQ_{ATTO594}$ to study internalization and the role of arrestins is particularly apposite here as there is now compelling evidence to suggest that agonists biased away from arrestin recruitment produce analgesia without the development of tolerance, a game changer in the development of analgesics for chronic pain.

Moreover, it is also possible to measure the ligand receptor interaction process in a FRET-based assay coupling the ATTO-labelled peptide with a GFP-labelled receptor in cell lines. This will also be possible in NOP-eGFP knock-in mice (Ozawa *et al.*, 2015).

In summary, we describe a novel ligand for use in the study of live-cell ligand–receptor interaction and tracking movement of liganded cell surface receptors. Use of higher resolution confocal technologies will facilitate a more detailed study of the 'unbinding' and recycling process.

Interesting further possibilities for this new ligand include its use in (i) brain sections and (ii) receptor binding protocols where the fluorescent label totally replaces the radioligand; this would revolutionize binding methodology for this receptor and potentially other members of the opioid family.

Acknowledgements

This study is funded by Biotechnology and Biological Sciences Research Council (BB/N000188/1). We thank the Advanced Imaging Facility (Dr K Straatman) at the University of Leicester for their support.

Author contributions

M.F.B. collected and analysed the data and wrote the paper. R.G. designed and synthesised the ligand and wrote the paper. J.M.W. and J.P.T. wrote the paper and obtained funding. G.C. designed the ligand and wrote the paper. D.G.L. analysed the data, wrote the paper and obtained funding.

Conflict of interest

The authors declare no conflicts of interest.

Declaration of transparency and scientific rigour

This Declaration acknowledges that this paper adheres to the principles for transparent reporting and scientific rigour of preclinical research recommended by funding agencies, publishers and other organisations engaged with supporting research.

References

Ahmadi F, Dabirian S, Faizi M, Tabatabai SA, Beiki D, Shahhosseini S (2014). Optimum conditions of radioligand receptor binding assay of ligands of benzodiazepine receptors. Iran J Pharm Res: IJPR 13: 79–86.

Al-Hashimi M, Scott SWM, Thompson JP, Lambert DG (2013). Opioids and immune modulation: more questions than answers. BJA: Br J Anaesth 111: 80–88.

Al-Hashimi M, McDonald J, Thompson JP, Lambert DG (2016). Evidence for nociceptin/orphanin FQ (NOP) but not μ (MOP), δ (DOP) or κ (KOP) opioid receptor mRNA in whole human blood. BJA: Br J Anaesth 116: 423–429.

Alexander SPH, Christopoulos A, Davenport AP, Kelly E, Marrion NV, Peters JA *et al*. (2017). The concise guide to pharmacology 2017/18: G protein-coupled receptors. Br J Pharmacol 174: S17–S129.

Arttamangkul S, Alvarez-Maubecin V, Thomas G, Williams JT, Grandy DK (2000). Binding and internalization of fluorescent opioid peptide conjugates in living cells. Mol Pharmacol 58: 1570–1580.

Barnes TA, McDonald J, Rowbotham DJ, Duarte TL, Lambert DG (2007). Effects of receptor density on nociceptin/orphanin FQ peptide receptor desensitisation: studies using the ecdysone inducible expression system. Naunyn Schmiedebergs Arch Pharmacol 376: 217–225.

Berahovich RD, Penfold ME, Schall TJ (2010). Nonspecific CXCR7 antibodies. Immunol Lett 133: 112–114.

Bird MF, Vardanyan RS, Hruby VJ, Calo G, Guerrini R, Salvadori S *et al*. (2015). Development and characterisation of novel fentanyl-δ opioid receptor antagonist based bivalent ligands. Br J Anaesth 114: 646–656.

Bird MF, Cerlesi MC, Brown M, Malfacini D, Vezzi V, Molinari P *et al*. (2016). Characterisation of the novel mixed μ-NOP peptide ligand dermorphin-N/OFQ (DeNo). PLoS One 11: e0156897.

Burgess A, Vigneron S, Brioudes E, Labbe JC, Lorca T, Castro A (2010). Loss of human greatwall results in G2 arrest and multiple mitotic defects due to deregulation of the cyclin B-Cdc2/PP2A balance. Proc Natl Acad Sci U S A 107: 12564–12569.

Camarda V, Calo G (2013). Chimeric G proteins in fluorimetric calcium assays: experience with opioid receptors. Methods Mol Biol (Clifton, NJ) 937: 293–306.

Cecyre B, Thomas S, Ptito M, Casanova C, Bouchard JF (2014). Evaluation of the specificity of antibodies raised against cannabinoid receptor type 2 in the mouse retina. Naunyn Schmiedebergs Arch Pharmacol 387: 175–184.

Ding H, Hayashida K, Suto T, Sukhtankar DD, Kimura M, Mendenhall V*et al*. (2015). Supraspinal actions of nociceptin/orphanin FQ, morphine and substance P in regulating pain and itch in non-human primates. Br J Pharmacol 172: 3302–3312.

Evans RM, You H, Hameed S, Altier C, Mezghrani A, Bourinet E *et al*. (2010). Heterodimerization of ORL1 and opioid receptors and its consequences for N-type calcium channel regulation. J Biol Chem 285: 1032–1040.

Franchi S, Moretti S, Castelli M, Lattuada D, Scavullo C, Panerai AE *et al*. (2012). Mu opioid receptor activation modulates Toll like receptor 4 in murine macrophages. Brain Behav Immun 26: 480–488.

Guerrini R, Calo G, Rizzi A, Bigoni R, Bianchi C, Salvadori S *et al*. (1998). A new selective antagonist of the nociceptin receptor. Br J Pharmacol 123: 163–165.

Guo Y, Xiao P, Lei S, Deng F, Xiao GG, Liu Y*et al*. (2008). How is mRNA expression predictive for protein expression? A correlation study on human circulating monocytes. Acta Biochim Biophys Sin 40: 426–436.

Hamdani N, van der Velden J (2009). Lack of specificity of antibodies directed against human β-adrenergic receptors. Naunyn Schmiedebergs Arch Pharmacol 379: 403–407.

Harding SD, Sharman JL, Faccenda E, Southan C, Pawson AJ, Ireland S *et al*. (2018). The IUPHAR/BPS guide to pharmacology in 2018: updates and expansion to encompass the new guide to immunopharmacology. Nucleic Acids Res 46: D1091–D1106.

Hashiba E, Lambert DG, Farkas J, Toth G, Smith G (2002). Comparison of the binding of [3H]nociceptin/orphaninFQ(1–13) NH2, [3H]nociceptin/orphaninFQ(1–17) OH and [125I] Tyr14nociceptin/orphaninFQ(1–17) OH to recombinant human and native rat cerebrocortical nociceptin/orphanin FQ receptors. Neurosci Lett 328: 5–8.

Hashimoto Y, Calo G, Guerrini R, Smith G, Lambert DG (2002). Effects of chronic nociceptin/orphanin FQ exposure on cAMP accumulation and receptor density in Chinese hamster ovary cells expressing human nociceptin/orphanin FQ receptors. Eur J Pharmacol 449: 17–22.

Hutchinson MR, Shavit Y, Grace PM, Rice KC, Maier SF, Watkins LR (2011). Exploring the neuroimmunopharmacology of opioids: an integrative review of mechanisms of central immune signaling and their implications for opioid analgesia. Pharmacol Rev 63: 772–810.

Jensen BC, Swigart PM, Simpson PC (2009). Ten commercial antibodies for alpha-1-adrenergic receptor subtypes are nonspecific. Naunyn Schmiedebergs Arch Pharmacol 379: 409–412.

Kitayama M, McDonald J, Barnes TA, Calo G, Guerrini R, Rowbotham DJ *et al*. (2007). In vitro pharmacological characterisation of a novel cyclic nociceptin/orphanin FQ analogue c [Cys(7,10)]N/OFQ(1-13) NH (2). Naunyn Schmiedebergs Arch Pharmacol 375: 369–376.

Kruger C, Kothe L, Struppert A, Pietruck C, Simm A, Grond S (2006). Expression und function of the ORL-1 receptor on human leukocytes. Schmerz (Berlin, Germany) 20: 509–518.

Lambert DG (2008). The nociceptin/orphanin FQ receptor: a target with broad therapeutic potential. Nat Rev Drug Discov 7: 694–710.

Liang X, Liu R, Chen C, Ji F, Li T (2016). Opioid system modulates the immune function: a review. Transl Perioper Pain Med 1: 5–13.

Malfacini D, Ambrosio C, Gro' MC, Sbraccia M, Trapella C, Guerrini R *et al*. (2015). Pharmacological profile of nociceptin/orphanin FQ receptors interacting with G-proteins and β-arrestins 2. PLoS One 10: e0132865.

McDonald J, Barnes TA, Okawa H, Williams J, Calo G, Rowbotham DJ *et al*. (2003). Partial agonist behaviour depends upon the level of nociceptin/orphanin FQ receptor expression: studies using the ecdysone-inducible mammalian expression system. Br J Pharmacol 140: 61–70.

Meunier JC, Mollereau C, Toll L, Suaudeau C, Moisand C, Alvinerie P *et al*. (1995). Isolation and structure of the endogenous agonist of opioid receptor-like ORL1 receptor. Nature 377: 532–535.

Michel MC, Wieland T, Tsujimoto G (2009). How reliable are G-protein-coupled receptor antibodies? Naunyn Schmiedebergs Arch Pharmacol 379: 385–388.

Mollereau C, Mouledous L (2000). Tissue distribution of the opioid receptor-like (ORL1) receptor. Peptides 21: 907–917.

Niwa H, Rowbotham DJ, Lambert DG (2012). Evaluation of primary opioid receptor antibodies for use in western blotting. Br J Anaesth 108: 530–532.

Ozawa A, Brunori G, Mercatelli D, Wu J, Cippitelli A, Zou B *et al*. (2015). Knock-in mice with NOP-eGFP receptors identify receptor cellular and regional localization. J Neurosci 35: 11682–11693.

Peterson YK, Luttrell LM (2017). The diverse roles of arrestin scaffolds in G protein-coupled receptor signaling. Pharmacol Rev 69: 256–297.

Plein LM, Rittner HL (2018). Opioids and the immune system – friend or foe. Br J Pharmacol 175: 2717–2725.

Pradidarcheep W, Stallen J, Labruyere WT, Dabhoiwala NF, Michel MC, Lamers WH (2009). Lack of specificity of commercially available antisera against muscarinergic and adrenergic receptors. Naunyn Schmiedebergs Arch Pharmacol 379: 397–402.

Reinscheid RK, Nothacker HP, Bourson A, Ardati A, Henningsen RA, Bunzow JR *et al*. (1995). Orphanin FQ: a neuropeptide that activates an opioid like G protein-coupled receptor. Science 270: 792–794.

Scherrer G, Imamachi N, Cao YQ, Contet C, Mennicken F, O'Donnell D *et al*. (2009). Dissociation of the opioid receptor mechanisms that control mechanical and heat pain. Cell 137: 1148–1159.

Schroder W, Lambert DG, Ko MC, Koch T (2014). Functional plasticity of the N/OFQ-NOP receptor system determines analgesic properties of NOP receptor agonists. Br J Pharmacol 171: 3777–3800.

Singh S, Sullo N, Bradding P, Agostino B, Brightling C, Lambert D (2013). Role of nociceptin orphanin FQ peptide – receptor system in mast cell migration. Eur Respir J 42.

Singh SR, Sullo N, Matteis M, Spaziano G, McDonald J, Saunders R *et al*. (2016). Nociceptin/orphanin FQ (N/OFQ) modulates immunopathology and airway hyperresponsiveness representing a novel target for the treatment of asthma. Br J Pharmacol 173: 1286–1301.

Slowe SJ, Clarke S, Lena I, Goody RJ, Lattanzi R, Negri L *et al*. (2001). Autoradiographic mapping of the opioid receptor-like 1 (ORL1) receptor in the brains of μ-, δ- or κ-opioid receptor knockout mice. Neuroscience 106: 469–480.

Snapp EL, Hegde RS (2006). Rational design and evaluation of FRET experiments to measure protein proximities in cells. Curr Protoc Cell Biol Chapter 17**:** Unit 17 19.

Strober W (2001). Trypan blue exclusion test of cell viability. Curr Protoc Immunol Appendix 3**:** Appendix 3B.

Talmont F, Mouledous L (2014). Evaluation of commercial antibodies against human sphingosine-1-phosphate receptor 1. Naunyn Schmiedebergs Arch Pharmacol 387: 427–431.

Thompson JP, Serrano-Gomez A, McDonald J, Ladak N, Bowrey S, Lambert DG (2013). The nociceptin/orphanin FQ system is modulated in patients admitted to ICU with sepsis and after cardiopulmonary bypass. PloS One 8: e76682.

Vallejo R, de Leon-Casasola O, Benyamin R (2004). Opioid therapy and immunosuppression: a review. Am J Ther 11: 354–365.

Wallrabe H, Elangovan M, Burchard A, Periasamy A, Barroso M (2003). Confocal FRET microscopy to measure clustering of ligand-receptor complexes in endocytic membranes. Biophys J 85: 559–571.

Williams JT, Ingram SL, Henderson G, Chavkin C, von Zastrow M, Schulz S *et al*. (2013). Regulation of mu-opioid receptors: desensitization, phosphorylation, internalization, and tolerance. Pharmacol Rev 65: 223–254.

Zhang L, Stuber F, Stamer UM (2013). Inflammatory mediators influence the expression of nociceptin and its receptor in human whole blood cultures. PloS One 8: e74138.

Supporting Information

Additional supporting information may be found online in the Supporting Information section at the end of the article.

https://doi.org/10.1111/bph.14504

Data S1 Chemistry.
Figure S1 Analytical HPLC profile of the [Cys(ATTO 594)^{18}] N/OFQ-NH_2 reaction mixture.
Figure S2 Analytical HPLC profile of the purified [Cys(ATTO 594)^{18}]N/OFQ-NH_2.
Figure S3 Mass spectrum of the purified [Cys(ATTO 594)^{18}] N/OFQ-NH_2.
Figure S4 A limited image z-series stack for 100 nM N/$OFQ_{ATTO594}$ binding to PMN is presented, panel A. In panel B, representative 'slices' at top, middle and bottom are shown.
Video S1 N/$OFQ_{ATTO594}$ binding and increased Ca^{2+} at 4°C.